Comparison of stress manifold and invariant manifold for reduced order modeling of thin structures

Yichang Shen*, Natacha Béreux*, Attilio Frangi◇ and Cyril Touzé*
* *IMSIA, Institut of Mechanical Sciences and Industrial Applications, ENSTA Paris, CNRS, EDF, CEA, Institut Polytechnique de Paris, Palaiseau, France.*
◇*Departement of Civil and Environmental Engineering, Politecnico di Milano, Milano, Italy.*

Summary. This article is devoted to the derivation of reduced-order models (ROMs) for geometrically nonlinear structure. A particular emphasis is put on comparing the Implicit condensation and expansion (ICE) method, which gives rise to a stress manifold to derive a reduced basis, with the invariant manifold defining a nonlinear normal mode (NNM). When the nonlinear stiffness coefficients are fully known, the ICE method reduces to a standard static condensation. Unfortunately, computing all the nonlinear (modal) coupling coefficients is not at hand when dealing with discretization methods based on the Finite Element (FE) procedure. The main advantage of the ICE method is thus to perform implicitely the static condensation, without the need of computing the coefficients. But the drawback is that the method will not, in any case, produce a better estimation than what can be obtained with an explicit static condensation. In particular, it is shown that the stress manifold tends to the invariant manifold only when a slow/fast decomposition of the system can be assumed.

Introduction

Thin and lightweight structures are prone to experience large amplitude vibrations, thus giving rise easily to geometric nonlinearity. As a consequence, the dynamics of the system is much more complex and the need to derive efficient reduced-order models (ROMs) more important.
When the spatial discretization of the structure is realized via the finite element method (FEM), specific problems arise due to the calculation of the nonlinear restoring force. To efficiently compute the reduced nonlinear internal forces, nonlinear ROM techniques for FE structures are generally classified into intrusive and non-intrusive methods. Non-intrusive methods take advantage of the usual outputs of any commercial FE code in order to derive, from algebraic operations on these, the coefficients of the ROM [1]. On the other hand, intrusive methods need a fine knowledge of the computation since elementary calculations are prescribed at the level of the element [2]. A widely used non-intrusive approach is the Stiffness Evaluation Procedure (StEP) method, which was first proposed by Muravyov and Rizzi [3]. In this method, one can directly retrieve the modal nonlinear coupling coefficients by prescribing selected static displacements to the model [4, 5]. On the other hand, another method relies on the use of static applied loads instead of prescribed displacements, and has been termed as the implicit condensation and expansion (ICE) method [6]. From the loadings and resulting large-amplitude displacements, a so-called stress manifold can be constructed in order to reduce the dynamics [7].
This main goal of the paper is to compare the ICE method to the invariant manifold proposed by Shaw and Pierre in order to define an NNM [8]. Invariant manifold theory is an efficient tool for interpreting many nonlinear dynamical phenomena. The article is structured as follows: Section 2 is devoted to explaining the ICE method and the invariant manifold approach. It is then shown in a general framework that if one assumes a slow/fast decomposition between the master and slave coordinates, then the static condensation approach reduces to the invariant manifold approach, at the leading order. Section 3 confirms these general findings by simplifying to a two degrees-of-freedom (dofs) system, for which explicit analytical expressions can be derived by asymptotic expansions, leading to an accurate term-by-term comparison. Section 4 extends the results to the case of continuous structures.

Framework

In this study, we restrict ourselves to the dynamics of thin and lightweight structures experiencing large amplitude vibrations, discretized using the FE procedure. Consequently our starting point is a semi-discrete equation of motion written for each degrees-of-freedom of the mesh used to space discretize the system, reading :

$$\mathbf{M}\ddot{\mathbf{q}} + \mathbf{K}\mathbf{q} + \mathbf{\Gamma}(\mathbf{q}) = \mathbf{F}, \tag{1}$$

with $\mathbf{M}$ the mass matrix arising from the FE discretization, $\mathbf{K}$ the linear stiffness matrix, $\mathbf{q}$ the vector of generalized displacements (displacements at the nodes) with dimension N, $\mathbf{F}$ the external forcing, and $\mathbf{\Gamma}(\mathbf{q})$ the nonlinear part of the stiffness. The modal basis is given by the combination of eigenvectors ϕ_i and eigenfrequencies ω_i verifying

$$\mathbf{K}\phi_i = \omega_i^2 \mathbf{M}\phi_i. \tag{2}$$

By using the linear change of coordinates $\mathbf{q} = \Phi\mathbf{X}$, with Φ the matrix of eigenvectors and $\mathbf{X}$ the modal coordinates, the equations of the motion in the modal basis read :

$$\ddot{X}_p + \omega_p^2 X_p + \sum_{i=1}^{+\infty}\sum_{j\geq i}^{+\infty} \alpha_{ij}^p X_i X_j + \sum_{i=1}^{+\infty}\sum_{j\geq i}^{+\infty}\sum_{k\geq j}^{+\infty} \beta_{ijk}^p X_i X_j X_k = 0, \tag{3}$$

This explicit formulation makes appear the quadratic and cubic nonlinear coupling coefficients α_{ij}^p and β_{ijk}^p, however for the sake of brevity the equations of motion in modal space will also be written as

$$\ddot{X}_p + \omega_p^2 X_p + f_p(X_1, X_2, ..., X_N) = 0. \tag{4}$$

ICE method

In the ICE method, the nonlinear restoring force is determined from a set of applied forces, which are generally selected as being colinear to the master modes. The procedure gives rise to a stress manifold [7], relating the slave displacements to the master ones by a functional relationship that has to be fitted from the outputs of the static solutions obtained. In particular, the relationship involves displacements only, and not the velocity, a distinctive feature from the invariant manifold. It is worth noticing that when the equation of motions are fully known, then the method is strictly equivalent to a usual explicit condensation. Consequently, in order to derive analytical expressions to compare with NNMs, the static condensation is here used. With the equations of motion of the system in the modal basis given by Eq.(4), let us separate the unknowns betwwen the master coordinates $X_1, ..., X_m$ and the slave coordinates $X_{m+1}, ..., X_s, ..., X_N$ with N the number of degrees of freedom (dofs). The master coordinates are the ones that are selected to derive the ROM while the slave coordinates are those one wants to cancel out in a correct way. Static condensation consists in finding functional relationships of the form

$$X_s = c_s(X_1, ..., X_m) \tag{5}$$

that define the stress manifold, for all $s \in [m+1, N]$, by simply neglecting the inertia of the slave coordinates. Hence the unknown functions c_s are found from the following equations, for $s \in [m+1, N]$:

$$\omega_s^2 c_s(X_1, ..., X_m) + f_s(X_1, ..., X_m, c_{m+1}(X_1, ..., X_m), ..., c_N(X_1, ..., X_m)) = 0. \tag{6}$$

then, the reduced-order models for the master coordinates reads :

$$\forall\, t \in [1, m], \quad \ddot{X}_t + \omega_t^2 X_t + f_t(X_1, ..., X_m, c_{m+1}(X_1, ..., X_m), ..., c_N(X_1, ..., X_m)) = 0. \tag{7}$$

When the full expressions of the functions f_s are not explicitely known, the functions c_s can be determined from a set of static solutions with increasing values of an imposed external force. Then a fitting procedure is needed to extrapolate the functional relationships from the generated data. The amplitudes of the imposed forcings, as well as the order of the fitting functions are also unknowns that have to be selected with care.

Invariant manifold

Nonlinear normal modes have been defined as invariant manifold in phase space by Shaw and Pierre [8, 9]. They can be computed thanks to the center manifold theorem [8, 9] or the normal form method [10]. In this contribution we select the invariant manifold approach in order to draw out the comparison with the ICE method. A relationship between the slave and master coordinates including both displacements X_p and velocities $Y_p = \dot{X}_p$, is assumed. The unknown are thus the functions h_1^s and h_2^s such that $X_s = h_1^s(X_1, Y_1, ..., X_m, Y_m)$, and $Y_s = h_2^s(X_1, Y_1, ..., X_m, Y_m)$, for $s \in [m+1, N]$. Following the general method of the invariant manifold, the unknown functions are solutions of the following partial differential equations that describe the geometry of the invariant manifold in phase space:

$$\sum_{i=1}^{m} \frac{\partial h_1^s}{\partial X_i} Y_i + \frac{\partial h_1^s}{\partial Y_i}\left[-\omega_i^2 X_i - f_i\right] = h_2^s, \quad \sum_{i=1}^{m} \frac{\partial h_2^s}{\partial X_i} Y_i + \frac{\partial h_2^s}{\partial Y_i}\left[-\omega_i^2 X_i - f_i\right] = -\omega_s^2 h_1^s - f_s. \tag{8}$$

The general solution of these equations is difficult to compute and can be achieved via asymptotic expansions or numerical methods. Once the unknown functions h_1^s and h_2^s have been obtained, the dynamics of the ROM are expressed as:

$$\forall\, t \in [1, m], \quad \ddot{X}_t + \omega_t^2 X_t + f_t(X_1, ..., X_m, h_1^{m+1}(X_1, Y_1, ..., X_m, Y_m), ..., h_1^N(X_1, Y_1, ..., X_m, Y_m)) = 0. \tag{9}$$

Comparison of stress manifold and invariant manifold

Let us assume that there is a slow/fast decomposition of the system, which means that the eigenfrequency ω_t of the master coordinates X_t, for $t \in [1, m]$, is much smaller than those of the slave coordinates X_s, for $s \in [m+1, N]$, i.e. $\omega_t \ll \omega_s$. This scaling can be reported into the equations of motion thanks to a small parameter ε. In order to express that the slave coordinates are much more stiff (thus corresponding to fast oscillations), the dynamics of the system Eq. (8), can be rewritten as:

$$\forall\, t \in [1, m], \quad \ddot{X}_t + \omega_t^2 X_t + f_t(X_1, X_2, ..., X_N) = 0, \tag{10a}$$

$$\forall\, s \in [m+1, N], \quad \ddot{X}_s + \frac{1}{\varepsilon}\omega_s^2 X_s + \frac{1}{\varepsilon} f_s(X_1, X_2, ..., X_N) = 0. \tag{10b}$$

The equations describing the geometry of the invariant manifold, Eq. (8), rewritten with the slow/fast assumption, read:

$$\sum_{t=1}^{m} \left(\frac{\partial h_1^s}{\partial X_t} Y_t + \frac{\partial h_1^s}{\partial Y_t}\left[-\omega_t^2 X_t - f_t\right] \right) = h_2^s, \tag{11a}$$

$$\sum_{t=1}^{m} \left(\frac{\partial h_1^s}{\partial X_t} Y_t + \frac{\partial h_1^s}{\partial Y_t}\left[-\omega_t^2 X_t - f_t\right] \right) = -\frac{1}{\varepsilon}\omega_s^2 h_1^s - \frac{1}{\varepsilon} f_s. \tag{11b}$$

Form the above Eq. (11b), h_1^s is obtained by neglecting the ε terms thanks to the slow/fast assumption:

$$\forall\ s \in\ [m+1, N], \quad \omega_s^2 h_1^s(X_1, Y_1, ..., X_m, Y_m) + f_s\left(X_1, ..., X_m, h_1^{m+1}, ..., h_1^N\right) = 0. \tag{12}$$

This equation is completely equivalent to Eq. (6), which define the stress manifold. Hence, the function h_1^s shall tend to the c_s, obtained with the static condensation; the only difference being the dependence on the velocities of h_1^s. If one assumes that h_1^s does not depend on the velocities, i.e.$\forall\ t \in\ [1, m]$, $\partial h_1^s / \partial Y_t = 0$, then the solutions are fully equivalent, and this can be used to derive another approximation regarding h_2^s as:

$$h_2^s = \sum_{t=1}^{m} \frac{\partial h_1^s}{\partial X_t} Y_t. \tag{13}$$

This last relationhsips shows that, under the above assumptions, a simple relation holds between the two functions h_1^s and h_2^s defining the invariant manifold, in line with the displacement/velocity dependence of the initial system. More generally, this simple derivation underline that stress manifold should tend to the invariant manifold, only if a slow/fast assumption exist, which is in the line of previously reported results, see *e.g.* [11]. However, if the slave modes are not stiff enough as compared to the master modes, then the ICE method may lose it accuracy, and using invariant manifolds in order to derive efficient ROMs would be a better choice.

Type of nonlinearity

Now we are comparing the prediction of the type of nonlinearity between these two methods, defined as the hardening/softening behaviour. In fact, one of the key points is whether a method can correctly predict the backbone curve of a nonlinear oscillator, and reduced-order models can give a correct prediction at least to the first order. To that purpose, let us assume that there is a single master coordinate X_p, and all other coordinates for $s \neq p$ are vanishing. The ROM will then consist of a single oscillator equation from which the type of nonlinearity can be derived. Also, if the single nonlinear oscillator equation is truncated to the cubic order [10, 12], a perturbative solution aloows one deriving an analytical expression for the leading order term which dictates the hardening/softening behaviour. Consequently, the general equations describing the stress manifolds, the invariant manifolds, and the dynamics within them, can be truncated up to order three.

In the case of static condensation, the leading order term for Eq. (5) for all $s \neq p$ reads

$$X_s = c_s(X_p) \simeq -\frac{\alpha_{pp}^s}{\omega_s^2} X_p^2 + \mathcal{O}(X_p^3), \tag{14}$$

such that the dynamics of the master mode on the stress manifold is expressed as

$$\ddot{X}_p + \omega_p^2 X_p + \alpha_{pp}^p X_p^2 + \left(\beta_{ppp}^p - \sum_{\substack{s=1 \\ s\neq p}}^{N} \frac{\alpha_{ps}^p \alpha_{pp}^s}{\omega_s^2}\right) X_p^3 + \mathcal{O}(X_p^4) = 0. \tag{15}$$

The frequency-amplitude relationship can be derived from this equation by a perturbative approach, see *e.g.*[10, 12], leading to the following generic formula,

$$\omega_{\mathrm{NL}} = \omega_p \left(1 + \Gamma a^2\right), \tag{16}$$

where ω_{NL} is the nonlinear frequency, depending on amplitude a, and Γ is the coefficient defining the type of nonlinearity. More specifically, positive values of Γ leads to a hardening type behaviour, while negative values means a softening behaviour is at hand. The type of nonlinearity for the static condensation approximation Γ_{SC} reads

$$\Gamma_{\mathrm{SC}} = \frac{1}{8\omega_p^2}\left(3\alpha_{ppp}^p - \frac{10(\alpha_{pp}^p)^2}{3\omega_p^2} - \sum_{\substack{s=1 \\ s\neq p}}^{N} \frac{3\alpha_{ps}^p \alpha_{pp}^s}{\omega_s^2}\right). \tag{17}$$

In the case of the invariant manifold approach, the individual expressions of slave coordinate can be found in [9, 13, 14], with the assumption of a single master NNM, for all $s \neq p$, and up to the second order, the formulas read as:

$$X_s = h_1^s(X_p, Y_p) = A_{s,1}^p X_p^2 + A_{s,2}^p X_p Y_p + A_{s,3}^p Y_p^2, \tag{18a}$$

$$Y_s = h_2^s(X_p, Y_p) = A_{s,4}^p X_p^2 + A_{s,5}^p X_p Y_p + A_{s,5}^2 Y_p^2, \tag{18b}$$

where

$$A^p_{s,1} = \frac{(\omega_s^2 - 2\omega_p^2)}{\omega_s^2(4\omega_p^2 - \omega_s^2)}\alpha^s_{pp}, \tag{19a}$$

$$A^p_{s,3} = \frac{-2}{\omega_s^2(4\omega_p^2 - \omega_s^2)}\alpha^s_{pp}, \tag{19b}$$

$$A^p_{s,5} = \frac{2}{4\omega_p^2 - \omega_s^2}\alpha^s_{pp}, \tag{19c}$$

$$A^p_{s,2} = A^p_{s,4} = A^p_{s,6} = 0. \tag{19d}$$

The reduced-order dynamics on the invariant manifold writes

$$\ddot{X}_p + \omega_p^2 X_p + \alpha^p_{pp} X_p^2 + \left(\beta^p_{ppp} + \sum_{\substack{s=1\\ s\neq p}}^{N} \alpha^p_{ps} A^p_{s,1}\right) X_p^3 + \sum_{\substack{s=1\\ s\neq p}}^{N} \alpha^p_{ps} A^p_{s,3} X_p Y_p^2 = 0. \tag{20}$$

The type of nonlinearity Γ_{IM} for the invariant manifold approach reads:

$$\Gamma_{\mathrm{IM}} = \frac{1}{8\omega_p^2}\left(3\beta^p_{ppp} - \frac{10(\alpha^p_{pp})^2}{3\omega_1^2} - \sum_{\substack{s=1\\ s\neq p}}^{N} \frac{3\omega_s^2 - 8\omega_p^2}{\omega_s^2 - 4\omega_p^2}\frac{\alpha^p_{ps}\alpha^s_{pp}}{\omega_s^2}\right). \tag{21}$$

Comparing the two predictions given by Eqs. (17) and (21), it is shown that the static condensation does not take into account 2:1 internal resonance. The formula obtained from the invariant manifold approach is correct, mainly because the reduction subspace is an NNM having the property of invariance embedded in its definition so that trajectories simulated in the reduced subspace also exist for the complete system. These facts have already been underlined in general studies concerned with the correct prediction of the type of nonlinearity, see *e.g.* [10, 18, 19, 20]. It is worthy to notice that if for all s, $\omega_s \gg \omega_p$, then the Γ_{IM} and Γ_{SC} would return equivalent value. This indicates that the static condensation approach gives reliable result only when the slow/fast decomposition is at hand.

Results on two-dofs systems

General results

In this section, we illustrate the general findings on the simplified case of a two degrees-of-freedom (dofs) system, having only two coordinates X_1 and X_2, with X_1 selected as the master coordinate and X_2 as the slave one. The idea is that under such a simplification, asymptotic expansions are easier to handle and one is able to give more insights to the general formula given just above, and explain in more detail how the static condensation will tend to the invariant manifold approach under the slow/fast assumption. All expansions are compared up to the third-order for consistency.
The nonlinear internal force in Eq. (4) for $p = 1,\ 2$ now reads:

$$f_p(X_1, X_2) = \alpha^p_{11}X_1^2 + \alpha^p_{12}X_1X_2 + \alpha^p_{22}X_2^2 + \beta^p_{111}X_1^3 + \beta^p_{112}X_1^2X_2 + \beta^p_{122}X_1X_2^2 + \beta^p_{222}X_2^3. \tag{22}$$

Assuming that X_1 is the master coordinate and X_2 the slave and applying static condensation, the relationship $X_2 = c(X_1)$ can be rewritten as:

$$\omega_2^2 c(X_1) + \alpha^2_{11}X_1^2 + \alpha^2_{12}X_1c(X_1) + \alpha^2_{22}c(X_1)^2 + \beta^2_{111}X_1^3 + \beta^2_{112}X_1^2c(X_1) + \beta^2_{122}X_1c(X_1)^2 + \beta^2_{222}c(X_1)^3 = 0. \tag{23}$$

The solution for c can be found based on an asymptotic expansion:

$$X_2 = c(X_1) = k_2X_1^2 + k_3X_1^3 + \mathcal{O}(X^3), \tag{24}$$

which is stopped here at order 3 but no maximal order of the polynomial expansion can be inferred from Eq. (24). A direct analytical solution for the k_i coefficients are computed by term-by-term identification of the coefficients of same power. The quadratic and cubic coefficients read:

$$k_2 = \frac{-\alpha^2_{11}}{\omega_2^2}, \tag{25a}$$

$$k_3 = \frac{-\beta^2_{111}\omega_2^2 + \alpha^2_{12}\alpha^2_{11}}{\omega_2^4}. \tag{25b}$$

Thus, the geometry of the stress manifold up to cubic terms is given by:

$$X_2 = c(X_1) = \frac{-\alpha^2_{11}}{\omega_2^2}X_1^2 + \frac{-\beta^2_{111}\omega_2^2 + \alpha^2_{12}\alpha^2_{11}}{\omega_2^4}X_1^3 \tag{26}$$

For the invariant manifolds, general expressions for the coefficients of the asymptotic expansions have already been derived in [9, 13, 14]. The two unknown functions describing the geometry of the invariant manifold can be written up to order three as:

$$X_2 = h_1(X_1, Y_1) = A^1_{11}X_1^2 + A^1_{12}X_1Y_1 + A^1_{22}Y_1^2 + B^1_{111}X_1^3 + B^1_{112}X_1^2Y_1 + B^1_{122}X_1Y_1^2 + B^1_{222}Y_1^3, \tag{27a}$$

$$Y_2 = h_2(X_1, Y_1) = A^2_{11}X_1^2 + A^2_{12}X_1Y_1 + A^2_{22}Y_1^2 + B^2_{111}X_1^3 + B^2_{112}X_1^2Y_1 + B^2_{122}X_1Y_1^2 + B^2_{222}Y_1^3. \tag{27b}$$

where the full expressions for the quadratic terms and cubic terms are given by

$$A^1_{11} = \frac{(\omega_2^2 - 2\omega_1^2)}{\omega_2^2(4\omega_1^2 - \omega_2^2)}\alpha^2_{11}, \tag{28a}$$

$$A^1_{22} = \frac{-2}{\omega_2^2(4\omega_1^2 - \omega_2^2)}\alpha^2_{11}, \tag{28b}$$

$$A^2_{12} = \frac{2}{4\omega_1^2 - \omega_2^2}\alpha^2_{11}, \tag{28c}$$

$$A^1_{12} = A^2_{11} = A^2_{22} = 0, \tag{28d}$$

$$B^1_{111} = \frac{\omega_2^2(4\omega_1^2 - \omega_2^2)(7\omega_1^2 - \omega_2^2)\beta^2_{111} + (9\omega_1^2\omega_2^2 - 18\omega_1^4 - \omega_2^4)\alpha^2_{11}\alpha^2_{12} + (2\omega_2^4 - 12\omega_1^4 - 10\omega_1^2\omega_2^2)\alpha^1_{11}\alpha^2_{11}}{\omega_2^2(4\omega_1^2 - \omega_2^2)(\omega_2^2 - \omega_1^2)(\omega_2^2 - 9\omega_1^2)}, \tag{28e}$$

$$B^1_{122} = \frac{6\omega_2^2(4\omega_1^2 - \omega_2^2)\beta^2_{111} + (8\omega_2^2 - 18\omega_1^2)\alpha^2_{11}\alpha^2_{12} - 20\omega_2^2\alpha^1_{11}\alpha^2_{11}}{\omega_2^2(4\omega_1^2 - \omega_2^2)(\omega_2^2 - \omega_1^2)(\omega_2^2 - 9\omega_1^2)}, \tag{28f}$$

$$B^2_{112} = \frac{3\omega_2^2(4\omega_1^2 - \omega_2^2)(3\omega_1^2 - \omega_2^2)\beta^2_{111} + (11\omega_1^2\omega_2^2 - 3\omega_2^4 - 18\omega_1^4)\alpha^2_{11}\alpha^2_{12} - 10\omega_2^2(3\omega_1^2 - \omega_2^2)\alpha^1_{11}\alpha^2_{11}}{\omega_2^2(4\omega_1^2 - \omega_2^2)(\omega_2^2 - \omega_1^2)(\omega_2^2 - 9\omega_1^2)}, \tag{28g}$$

$$B^2_{222} = B^1_{122}, \tag{28h}$$

$$B^2_{111} = B^2_{122} = B^1_{112} = B^1_{222} = 0. \tag{28i}$$

The coefficients derived from the invariant manifold approach shows singularities when internal resonances exist between the eigenfrequencies, this feature is not retrieved by the static condensation. Also, the dependence on the eigenfrequencies is playing a much more important role in the expressions giving the geometry of the invariant manifold in phase space. If one assumes that $\omega_2 \gg \omega_1$, the nonlinear relationships between slave and master coordinates simplifies to :

$$X_2 = \frac{-\alpha^2_{11}}{\omega_2^2}X_1^2 + \frac{2\alpha^2_{11}}{\omega_2^4}Y_1^2 + \frac{-\omega_2^2\beta^2_{111} + \alpha^2_{12}\alpha^2_{11} - 2\alpha^1_{11}\alpha^2_{11}}{\omega_2^4}X_1^3 + \frac{6\omega_2^2\beta^2_{111} - 8\alpha^2_{11}\alpha^2_{12} + 20\alpha^1_{11}\alpha^2_{11}}{\omega_2^6}X_1Y_1^2, \tag{29a}$$

$$Y_2 = -\frac{2\alpha^2_{11}}{\omega_2^2}X_1Y_1 + \frac{-3\omega_2^2\beta^2_{111} + 3\alpha^2_{11}\alpha^2_{12} - 10\alpha^1_{11}\alpha^2_{11}}{\omega_2^4}X_1^2Y_1 + \frac{6\omega_2^2\beta^2_{111} - 8\alpha^2_{11}\alpha^2_{12} + 20\alpha^1_{11}\alpha^2_{11}}{\omega_2^6}Y_1^3. \tag{29b}$$

One can see that the quadratic terms in X_1^2 in Eqs. (26) and (29a) are exactly the same. The dependence on the velocity master variable Y_1 is not present for the stress manifold, however this dependence is proportional to $1/\omega_2^4$ in (29a) for the quadratic term in Y_1^2, one order of magnitude smaller than the term in X_1^2, scaling as $1/\omega_2^2$, and thus can be considered as negligible. The coefficients for the cubic term in X_1^3 are almost the same in the two expressions. Recalling that the slow/fast assumption should also hold for the nonlinear stiffness so that $\alpha^2_{12} \gg \alpha^1_{11}$ and rewriting the terms $\alpha^2_{12}\alpha^2_{11} - 2\alpha^1_{11}\alpha^2_{11})$ in the X_1^3 coefficient in (29a) as $\alpha^2_{11}(\alpha^2_{12} - 2\alpha^1_{11})$, one can therefore draw a conclusion that both X_1^3 coefficients tends to have the same values under the slow/fast assumption. Finally the last cubic term in $X_1Y_1^2$ in (29a) scales as $1/\omega_2^4$, which is also one order of magnitude smaller and can thus be neglected.

Consequently, the above comparison show that the results given by the static condensation tend to those given by the invariant manifold approach if a slow/fast decomposition holds. The dependence on the velocity is one order of magnitude smaller and thus tends to disappear. One can also observe that the Eq. (13) now specifying to

$$h_2 \simeq \frac{\partial h_1}{\partial X_1}Y_1, \tag{30}$$

also holds, if and only if one also assumes $\alpha^2_{12} \gg \alpha^1_{11}$, which is the case if the slow/fast dynamics is assumed.

Now, we are comparing the reduced-order dynamics given by the two methods up to order three. The dynamics of the master coordinate X_1 with the stress manifold is given by Eq. (7) and reads:

$$\ddot{X}_1 + \omega_1^2X_1 + \alpha^1_{11}X_1^2 + \left(\beta^1_{111} - \frac{\alpha^1_{12}\alpha^2_{11}}{\omega_2^2}\right)X_1^3 = 0. \tag{31}$$

The dynamics with the invariant manifold, with X_2 given by Eq. (29a), reads:

$$\ddot{X}_1 + \omega_1^2X_1 + \alpha^1_{11}X_1^2 + \left(\frac{(\omega_2^2 - 2\omega_1^2)}{\omega_2^2(4\omega_1^2 - \omega_2^2)}\alpha^1_{12}\alpha^2_{11} + \beta^1_{111}\right)X_1^3 + \left(\frac{-2}{\omega_2^2(4\omega_1^2 - \omega_2^2)}\alpha^1_{12}\alpha^2_{11}\right)X_1Y_1^2 = 0, \tag{32}$$

which simplifies to the following with $\omega_2 \gg \omega_1$:

$$\ddot{X}_1 + \omega_1^2 X_1 + \alpha_{11}^1 X_1^2 + \left(\beta_{111}^1 - \frac{\alpha_{12}^1 \alpha_{11}^2}{\omega_2^2}\right) X_1^3 + \frac{2\alpha_{12}^1 \alpha_{11}^2}{\omega_2^4} X_1 Y_1^2 = 0, \tag{33}$$

Comparing Eq. (33) with (31), one can observe that the cubic term in X_1^3 is the same, confirming again that the stress manifold gives reliable results only under the slow/fast assumption. The supplementary term in $X_1 Y_1^2$ for the invariant manifold is negligible because it scales as $1/\omega_2^4$.

Numerical results on a mass connected to two bars

In this section, we consider a two dofs system introduced in [10], consisting of a mass connected to two nonlinear bars and oscillating in the plane. In this case, the equation of motion contains quadratic and cubic terms. By using asymptotic expansions to derive the first terms of the solution of the invariant manifold and the static condensation, one can realize a term-by-term comparison and contrast the similarities between the two methods. The equations of motion read:

$$\begin{aligned}
&\ddot{X}_1 + \omega_1^2 X_1 + \frac{\omega_1^2}{2}(3X_1^2 + X_2^2) + \omega_2^2 X_1 X_2 + \frac{\omega_1^2 + \omega_2^2}{2} X_1 (X_1^2 + X_2^2) = 0, \\
&\ddot{X}_2 + \omega_2^2 X_2 + \frac{\omega_2^2}{2}(3X_2^2 + X_1^2) + \omega_1^2 X_1 X_2 + \frac{\omega_1^2 + \omega_2^2}{2} X_2 (X_1^2 + X_2^2) = 0.
\end{aligned} \tag{34}$$

The main goal of this section is to compare the results provided by the static condensation and those obtained with NNMs, in terms of the geometry of the manifold used to reduce the dynamics, and expression of the dynamics onto this reduced subspace.

By replacing α and β in Eq. (24) with known coefficients given in Eq. (34), the static condensation gives the following formula for the stress manifold up to the third order :

$$X_2 = c_2(X_1) = -\frac{1}{2} X_1^2 + \frac{\omega_1^2}{2\omega_2^2} X_1^3. \tag{35}$$

For the geometry of the manifolds, only focusing on $X_2 = h_1(X_1, Y_1)$ for comparison in the plane (X_1, X_2), the Eq. (27a) reads

$$X_2 = h_1(X_1, Y_1) = A_{11}^1 X_1^2 + A_{22}^1 Y_1^2 + B_{111}^1 X_1^3 + B_{122}^1 X_1 Y_1^2. \tag{36}$$

which is also stopped here at order 3 because the derivation of higher-order terms leads to difficult and lenghty expressions needing for a symbolic computation processor. The coefficients A_{11}^1, A_{22}^1, B_{111}^1 and B_{122}^1 are given below, together with their approximate value when one considers the slow/fast assumption $\omega_2 \gg \omega_1$:

$$\begin{aligned}
A_{11}^1 &= \frac{\omega_2^2 - 2\omega_1^2}{2(4\omega_1^2 - \omega_2^2)} \xrightarrow{\omega_2 \gg \omega_1} -\frac{1}{2}, \\
A_{22}^1 &= \frac{-1}{4\omega_1^2 - \omega_2^2} \xrightarrow{\omega_2 \gg \omega_1} \frac{1}{\omega_2^2}, \\
B_{111}^1 &= \frac{(\omega_2^4 - 18\omega_1^4 - 3\omega_1^2\omega_2^2)\omega_1^2\omega_2^2}{\omega_2^2(4\omega_1^2 - \omega_2^2)(\omega_2^2 - \omega_1^2)(\omega_2^2 - 9\omega_1^2)} \xrightarrow{\omega_2 \gg \omega_1} \frac{\omega_1^2}{-\omega_2^2}, \\
B_{122}^1 &= \frac{(-11\omega_2^2 - 9\omega_1^2)\omega_1^2\omega_2^2}{\omega_2^2(4\omega_1^2 - \omega_2^2)(\omega_2^2 - \omega_1^2)(\omega_2^2 - 9\omega_1^2)} \xrightarrow{\omega_2 \gg \omega_1} \frac{11\omega_1^2}{\omega_2^2}.
\end{aligned} \tag{37}$$

These expressions indicate that the invariant manifold method gives more general results that tends to retrieve those given by static condensation at the leading order only, when a slow/fast assumption holds. Substituting the values of the coefficients A_{11}^1, A_{22}^1, B_{111}^1 and B_{122}^1 obtained with the slow/fast asumption into Eq. (36), one obtains

$$X_2 = h_1(X_1, Y_1) \simeq -\frac{1}{2} X_1^2 + \frac{1}{\omega_2^2} Y_1^2 - \frac{\omega_1^2}{\omega_2^2} X_1^3 + \frac{11\omega_1^2}{\omega_2^2} X_1 Y_1^2, \tag{38}$$

which can be compared to Eq. (35) directly, showing that there are additional terms implying the velocities in the invariant manifold, and the cubic term in X_1^3 is not the same for the two methods, however, the differences are scaling according to $1/\omega_2^2$, thus these are negligible. Consequently, the leading order term is the first quadratic term in Eqs. (35) and (38) so that a cut of both stress and invariant manifold in the plane (X_1, X_2), and with slow/fast decomposition, should show a parabola scaling as $-\frac{1}{2} X_1^2$.

NLet us now compare the results given by the reduced-order dynamics. Of utmost importance for the ROM is its ability to correctly predict the backbone curve. Using static condensation up to order three, replacing the master coordinate X_2 by Eq. (35) and substutiting into Eq. (3), leads to the following reduced-order dynamics :

$$\ddot{X}_1 + \omega_1^2 X_1 + \frac{3\omega_1^2}{2} X_1^2 + \frac{\omega_1^2}{2} X_1^3 = 0. \tag{39}$$

This equation can be compared to the reduced dynamics given by the invariant manifold approach, by replacing the master coordinate X_2 by the relationship of $X_2 = h_1(X_1, Y_1)$, and also substutiting into Eq. (3), up to order 3 :

$$\ddot{X}_1 + \omega_1^2 X_1 + \frac{3\omega_1^2}{2} X_1^2 + \frac{\omega_1^2(4\omega_1^2 + \omega_2^2)}{2(4\omega_1^2 - \omega_2^2)} X_1^3 + \frac{\omega_2^2}{\omega_2^2 - 4\omega_1^2} X_1 Y_1^2 = 0. \tag{40}$$

Using now the slow/fast assumption in Eq. (40), one obtains :

$$\ddot{X}_1 + \omega_1^2 X_1 + \frac{3\omega_1^2}{2} X_1^2 - \frac{\omega_1^2}{2} X_1^3 + X_1 Y_1^2 = 0. \tag{41}$$

Comparing Eqs. (39) and (41), it is shown that even with the slow/fast assumption, the reduced-order dynamics given by the two methods are different. Again, the invariant manifold approach gives rise to velocity-dependent terms, contrary to the static condensation.

Now a comparison of the outcomes of the two methods will be discussed, since the dynamics produced by the two ROMs could be misleaded by a term-by-term comparison, it is better to focus on the prediction of the type of nonlinearity, as already exemplified in previous demonstration. Using the value of Γ_{SC} given in Eq. (17) and replacing the quadratic coefficients by their values, we obtained $\Gamma_{\mathrm{SC}} = -3/4$ for static condensation, *i.e.* a constant value that do not depend on the parameter of the system. On the other hand, using Eq. (21) shows that

$$\Gamma_{\mathrm{IM}} = \frac{-3\omega_1^2 + \omega_2^2}{4\omega_1^2 - \omega_2^2}. \tag{42}$$

Interestingly, the type of nonlinearity predicted by the IM approach has a divergence at the 2:1 internal resonance, a classical feature due to the strong coupling arising in the two modes in this region, and tends to -1 when $\omega_2 \gg \omega_1$. This means that a persistent error in the prediction of the type of nonlinearity is given by the static condensation even when the slow/fast assumption holds. This conclusion is a bit different from the one obtained in section , which is due to the particular values of the quadratic coefficients α_{ij}^p. Indeed, being fully dependent on ω_1 and ω_2, their relative values when applying the slow/fast assumption has a direct consequence on the results.

Fig. 1(a)-(d)-(g) compares the exact invariant manifold obtained by numerical continuation of periodic orbits to the stress manifold obtained with the exact static condensation. These figures clearly underline that the stress manifold is the same subspace than the invariant manifold when a slow/fast decomposition is at hand. However, even though the reduced dynamics is projected on the same subspace, the projection method is not strictly equivalent. Consequently the approximation of the oscillation frequency, given by the backbone curves in Fig. 1(c)-(f)-(i) do not tend to the same results.

Numerical examples on continuous structures

In order to better compare the two methods, a clamped-clamped beam discretized with the FE procedure, is investigated and reduced to a single mode is targeted. The dimensions of the beams are selected as: length $L = 1m$, width $b = 0.05m$, thickness $h = 0.001m$. Material properties are selected as: density $\rho = 7800kg/m^3$, Young modulus $E = 2.1e11pa$, and PoissonâĂŹs ratio $v = 0$ in order to better mimic the assumptions of the theory of beams. This assumption has been used (*e.g.* in [7]) when comparisons with theoretical results from beam theory are needed. The beam is discretized with 100 elements in the length and 4 elements in the width, to make sure the mesh of the FE model is small enough to has its first 10 eigenfrequencies converged. In this paper, the calculations have been realized with the open-source finite element software Code_aster, with DKT elements.

With the finite element model, a simple case of a single master mode (the fundamental flexural mode) is investigated for comparing between the ICE method and the NNM approach. The ICE method is derived by first applying a set of body forces to the structure, *i.e.* to Eq. (1), these load cases should be proportional to the first mode $\boldsymbol{F} = \lambda_1 \phi_1$ for varying values of the parameter λ_1, where ϕ_1 denotes the fundamental mode. From the displacement computed by the FE model, the modal displacements can be retrieved by projecting again along ϕ_1, so that a nonlinear relationship between the displacement and the scaling factors λ_1 is numerically obtained, and the nonlinear restoring force for the reduced-order model can be retrieved by fitting this relationship.

The fitting procedure for a single coordinate to construct the ROM by the ICE method is illustrated at the bottom right corner in Fig. 2. 50 values of λ_1 have been selected, where the load scales are chosen to obtain displacement in the range of ± 1.5 times of thickness. Such that the ROM given by the ICE method with a polynomial expansion is expressed as

$$\ddot{q}_1 + \omega_1^2 q_1 + \gamma_{111}^1 q_1^3 = F. \tag{43}$$

where γ_{111}^1 is obtained from the fitting procedure. Numerical results show that one obtains $\gamma_{111}^1 = 5.2310e + 09$. Here only the cubic term appears because of the symmetry reasons, since the beam is a flat, symmetric structure.

With the StEP method a converged reduced-order models based on the linear eigenmodes can be derived, see *e.g.* [15, 16, 17]. By using first flexural and 2nd, 4th and 6th in-plane modes as a basis, which is sufficient to ensure convergence, the associated quadratic and cubic coefficients can be computed. Quadratic coefficients appear due to the membrane/flexural

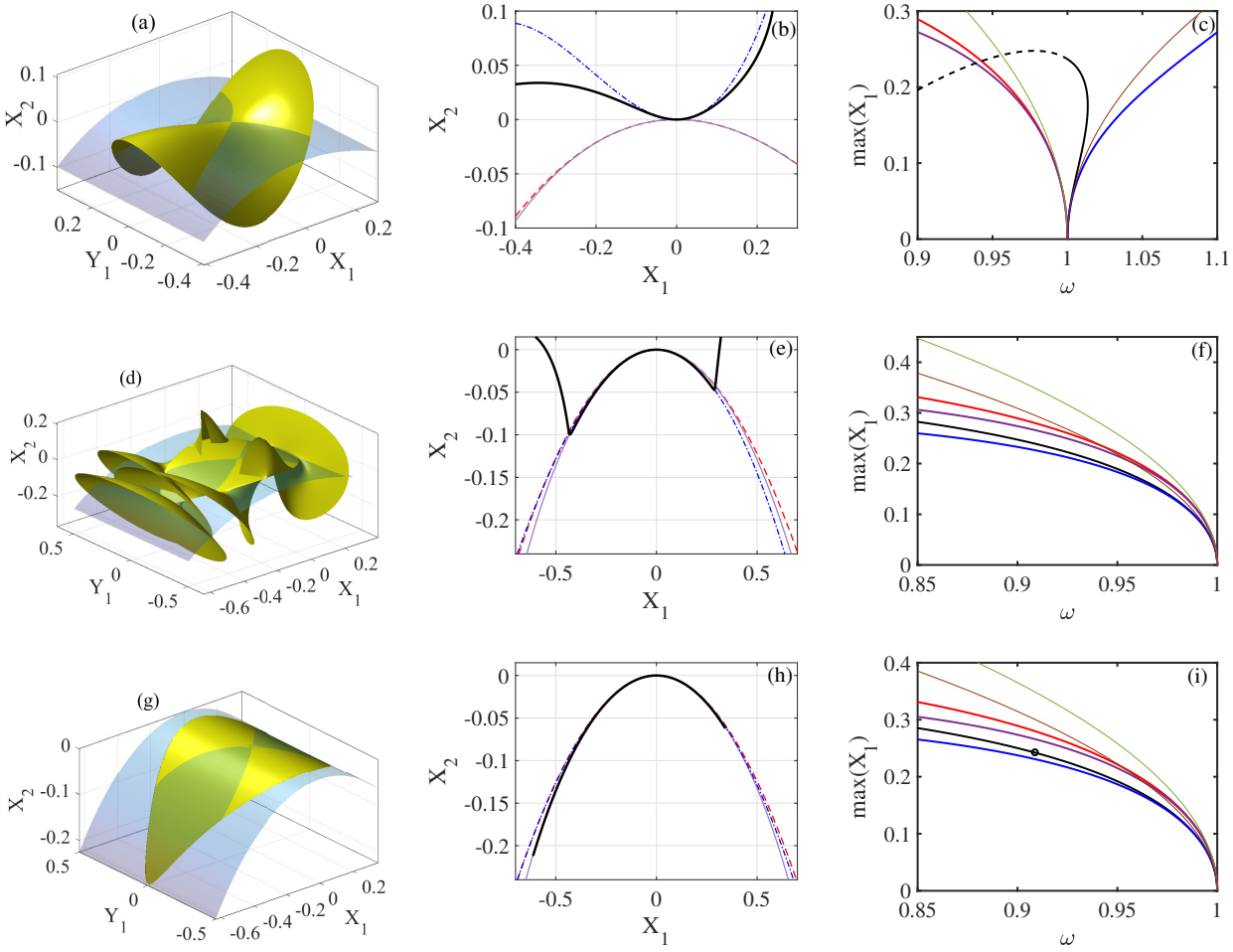

Figure 1: (a),(d),(g) Invariant manifold (yellow) in space (X_1, Y_1, X_2), compared with the exact stress manifold (blue). (b),(e),(h) Comparisons of stress and invariant manifolds in the plane (X_1, X_2) for the two-dofs system. The static condensation up to order 3 (red dashed) and up to order 9 (violet) is compared to the exact invariant manifold (black line) and its third-order analytical approximation (blue dash–dotted). (c),(f),(i) Comparison of backbone curves computed from the full model (black, unstable part in dashed line), the static condensation up to order 3 and 9 (red and purple) and the invariant manifold up to order three (blue). The first order of nonlinear frequency of the third order invariant manifold, Eq. (42) (brown curve), the first order of nonlinear frequency of the third order static condensation (green curve). (a)-(c) $\omega_{master} = 1$ and $\omega_{slave} = \sqrt{3.5}$. (d)-(f) $\omega_{master} = 1$ and $\omega_{slave} = 5$. (g)-(i) $\omega_{master} = 1$ and $\omega_{slave} = 10$.

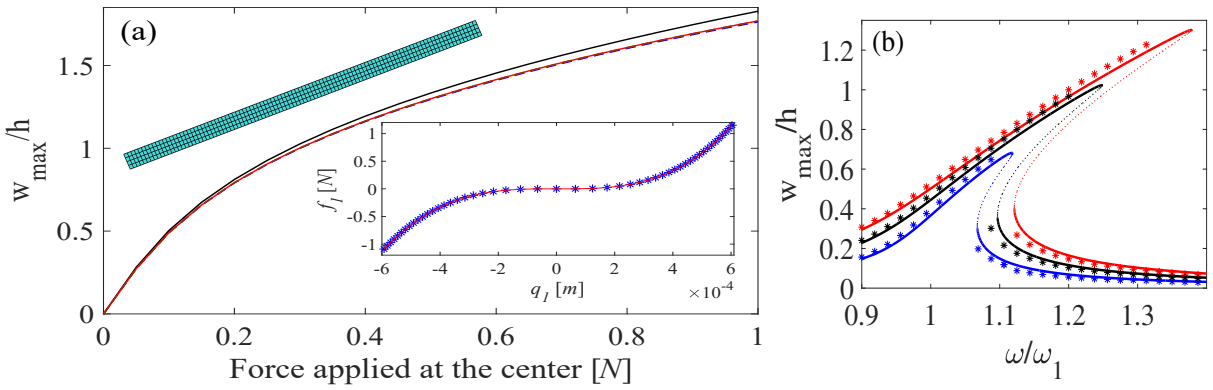

Figure 2: (a): Comparison of ROMs with FE solution for a clamped-clamped beam, statically excited at center with an increasing loading value. The FE solution (black line) is compared to three reduced order models: a single mode obtained with the ICE method (blue dashed line), a four mode projection using the SteP method (red line), and the reduction to a single NNM from this four mode solution (brown line). Upper left corner: The meshs in the FE model of the beam. Bottom right corner: illustration of the fitting procedure for the ICE method: blue stars represent the outputs obtained from static applied force on the FE model, red curve is the fitted polynomial of order 3. (b): Frequency response curves in the vicinity of the first eigenfrequency, for three different amplitudes of the forcing: 0.00525N (blue), 0.00875N (black), 0.01225N (red). The full line predictions of the ROM developed by the ICE method, given by Eq. (43), are obtained by numerical continuation, and is compared to direct time integration on the full FE model (stars).

coupling [15], and the first three of this family is sufficient to ensure convergence. Hence, from these known coefficients, a reduced-order model composed of this four eigenmodes can be constructed in order to reduce the dynamics to a single dof, the classical static condensation is applied to lead an equation in the form of Eq. (43),

$$\tilde{\gamma}^1_{111} = \beta^1_{111} - \sum_{p=2}^{4} \frac{\alpha^1_{1p}\alpha^p_{11}}{\omega^2_p}, \tag{44}$$

where the β and α are the nonlinear stiffness coefficients computed from the StEP method. The $\tilde{\gamma}_{111}$ is computed numerically to be $5.2308e+09$, showing in this case that the ROM built by implicit condensation is equivalent with explicit. Finally, on the ROM developed with the StEP method, one can apply the reduction to a single NNM, thus obtaining a reduced dynamics reading

$$\ddot{q}_1 + \omega_1^2 q_1 + \bar{\gamma}^1_{111} q_1^3 + B^1_{111} q_1 \dot{q}_1^2 = F. \tag{45}$$

The result of the coefficients are $\bar{\gamma}^1_{111} = 5.2308e+09$ and $B^1_{111} = 1.2506$. As expected, the three methods gives exactly the same results and in the frame of the previous demonstration. Indeed, in-plane modes are in very high eigenfrequencies so that the slow/fast assumption is at hand, thus, all the methods give the same results. In order to be more intuitive, Fig. 2 (a) illustrates a test with static concentrated force applied at the center of the beam. The maximum displacement, which is computed with the three single mode dynamics, agrees the result given by the full FE solution very well up to 1.5 times the thickness. Fig. 2 (b) shows nonlinear dynamical frequency response in the vicinity of the first eigenfrequency with a Rayleigh damping of the form $C_s = 1.34[M]$ has been selected, corresponding to a damping ratio of 2 percent for the first mode. The dotted points donates the corresponding full FE solution, computed by direct numerical integration. The response of the ROMs have been computed by numerical continuation using Manlab.

Conclusions

This paper addressed a comparison between implicit condensation and expansion (ICE) method and NNMs defined as invariant manifolds in phase space. The main advantage of the ICE method is to implicitely compute the static condensation of the slave degrees of freedom, without the need to compute all their couplings with the master variables. But the stress manifold produced by this method is not invariant and does not depend on the velocities, so that it can be safely used only if a slow/fast decompostion exists between slave and master coordinate. Another drawback of the ICE method also relies on the fitting procedure that is needed once the applied static loadings have been computed. Increasing the number of master modes makes this step more and more difficult and numerous problems arise in the accuracy of the obtained results. For all these reasons, ROMS built from general theorems from the dynamical systems theory, using invariant manifolds, seems to be more appropriate since they can be sued safely without extra assumptions (such as slow/fast separation), and without the tedious ftting procedure, see *e.g.* [21, 22].

References

[1] M. P. Mignolet, A. Przekop, S. A. Rizzi and S. M. Spottswood (2013) A review of indirect/non-intrusive reduced order modeling of nonlinear geometric structures. *Journal of Sound and Vibration*, **332**:2437-2460.

[2] C. Touzé, M. Vidrascu and D. Chapelle (2014) Direct finite element computation of non-linear modal coupling coefficients for reduced-order shell models. *Computational Mechanics*, **54**(2):567-580.

[3] A. A. Muravyov and S. A. Rizzi. (2003) Determination of nonlinear stiffness with application to random vibration of geometrically nonlinear structures. *Computers and Structures* **81**:1513-1523.

[4] M. Mignolet and C. Soize. (2008) Stochastic reduced-order models for uncertain geometrically nonlinear dynamical systems *Computer Methods in AppL. Mech. Engrg.* **197**:3951âĂŞ3963 .

[5] R. Perez, X. Q. Wang, and M. P. Mignolet. (2014) Nonintrusive Structural Dynamic Reduced Order Modeling for Large Deformations: Enhancements for Complex Structures. *J. Comput. Nonlinear Dynam.* **9**(3).

[6] J. J. Hollkamp and G. W. Gordon (2008) Reduced order models for nonlinear response prediction: Implicit condensation and expansion. *J. Sound. Vib* **318**(4):1139-1153.

[7] A. Frangi and G. Gobat (2019) Reduced order modelling of the non-linear stiffness in MEMS resonators. *Int. J. of Non-linear Mech.* **116**:211-218.

[8] S. W. Shaw and C. Pierre (1991) Non-linear normal modes and invariant manifolds, *J. Sound. Vib* **150(1)**:170-173.

[9] Shaw S.W. and Pierre C. (1993) Normal modes for nonlinear vibratory systems, *J. Sound. Vib* **150(1)**:85-124.

[10] C. Touzé, O. Thomas and A. Chaigne (2004) Hardening/softening behaviour in non-linear oscillations of structural systems using non-linear normal modes. *J. Sound. Vib* **273**(1-2): 77-101.

[11] G. Haller and S. Ponsioen (2017) Exact model reduction by slow/fast decomposition of nonlinear mechanical systems, *Nonlinear Dynam.* **90**:617-647.

[12] A. H. Nayfeh and D. T. Mook. (1979) Nonlinear oscillations. John Wiley & sons, NY.

[13] N. Boivin, C. Pierre, and S. Shaw. (1995) Non-linear normal modes, invariance, and modal dynamics approximations of non-linear systems., *Nonlinear Dynam.* **8**:315-346

[14] Pesheck, E. and Boivin, N. and Pierre, C. and Shaw, S. W. (2001) Nonlinear Modal Analysis of Structural Systems Using Multi-Mode Invariant Manifolds. *Nonlinear Dynam.* **25**(1):183-205.

[15] A. Givois, A. Grolet, O. Thomas, and J.-F. Deü. (2019) On the frequency response computation of geometrically nonlinear flat structures using reduced-order finite element models. *Nonlinear Dynam.*, **92**(2):1747âĂŞ1781.

[16] A. Vizzaccaro and A. Givois and P. Longobardi and Y. Shen and J.-F. Deü and L. Salles and C. Touzé and O. Thomas (2020), Non-intrusive reduced order modelling for the dynamics of geometrically nonlinear flat structures using three-dimensional finite elements. *Computational Mechanics*, submitted.

[17] C. S. M. Sombroek and P. Tiso and L. Renson and G. Kerschen (2018), Numerical computation of nonlinear normal modes in a modal derivative subspace *Computers and Structures*, **195**:34-46.

[18] C. Touzé and O. Thomas (2006), Non-linear behaviour of free-edge shallow spherical shells: effect of the geometry. *Int. J. of Non-linear Mech*, **41**(5): 678-692.

[19] W. Lacarbonara and G. Rega and A. H. Nayfeh (2000), Reduction methods for nonlinear vibrations of spatially continuous systems with initial curvature. *Solid Mechanics and its applications*, **77**: 235-246.

[20] H. N. Arafat and A. H. Nayfeh (2003), Non-linear responses of suspended cables to primary resonance excitation. *J. Sound. Vib* **266**: 325-354.

[21] Z. Veraszto and S. Ponsioen and G. Haller (2020), Explicit third-order model reduction formulas for general nonlinear mechanical systems, *Journal of Sound and Vibration*, **468**, 115039.

[22] A. Vizzaccaro, Y. Shen, L. Salles and C. Touzé (2020), Model order reduction methods based on normal form for geometrically nonlinear structures: a direct approach, *Proceedings of Euromech Non-linear Dynamics Conference, ENOC 2020*, Lyon.